RESEARCH PAPER

Activated flux TIG welding of titanium

H. C. Dey · S. K. Albert · A. K. Bhaduri ·
U. Kamachi Mudali

Abstract Metallurgical characterization and qualification of activated flux TIG (ATIG) weld joints of titanium produced using in-house developed activating flux are presented. The flux formulation was optimized after carrying out trials with different sets of flux powders and subsequent metallographic observation of weld bead profile. ATIG welding of titanium using this flux, with optimized welding parameters, produces full penetration welds in 6-mm-thick plates having weld bead depth-to-width ratio of 1.25 compared to 0.25 of conventional TIG welds. ATIG weld joints were prepared using 6-mm-thick titanium plates using square-butt joint geometry and these joints were qualified by radiography. Root and face bend tests passed 4T bend radius as per American Society of Mechanical Engineers (ASME) Boiler and Pressure Vessel Code-Section IX requirements with bend angle of 180°. Transverse tensile testing of weld joints showed fracture in the weld metal with sufficient ductility and tensile strength of 398 MPa, which was close to the base material tensile strength of 402 MPa thereby meeting ASME Section IX requirements. Uniform hardness across the weld confirmed that the weld was not contaminated by components of flux or atmospheric gases, which can result in increased hardness of the weld metal leading to embrittlement. The corrosion test of the weld joints in 11.5 M boiling nitric acid showed improved corrosion resistance compared to base material.

Keywords Active fluxes · Titanium · GTA welding · Butt joints · Mechanical properties · Corrosion tests

H. C. Dey · S. K. Albert · A. K. Bhaduri (✉) · U. K. Mudali
Indira Gandhi Centre for Atomic Research,
Kalpakkam 603102, India
e-mail: arunkbhaduri@gmail.com

1 Introduction

Titanium and its alloys are used primarily in corrosion resistance service and specific strength efficient structures. Commercially pure (CP) titanium is used for corrosion resistance applications fabricated into tanks, heat exchangers, chemical processing vessels, power generation plants, etc. However, titanium alloys are mostly used in high-performance service requirement like aerospace applications. In nuclear industries, CP titanium (ASTM grades 1 and 2) is used as a structural material for the reprocessing of spent fuel where highly concentrated nitric acid in boiling condition is used for the dissolution of spent fuel. Welding fabrication of titanium and its alloys are very much sensitive to atmospheric contamination by oxygen, nitrogen, and hydrogen and requires completely inert or vacuum environment to protect the weld metal and heat affected zone until the temperature drops below 773 K [1, 2]. The atmospheric contamination causes embrittlement and hardness increase with reduction in toughness and ductility of the weld joints. Further, titanium shows excessive grain growth at high temperature which is detrimental to weld toughness. The cleanliness of the weld joints including filler wire is critical to avoid weld contamination and porosity. Contaminations of the weld joints by iron reduce the corrosion resistance [1]. Therefore, fabrication of titanium equipments by welding needs special attention and weld joints needs to be qualified with all the tests intended for actual service condition.

The widely used fusion welding processes for joining titanium and its alloys are tungsten inert gas (TIG) welding, gas metal arc welding, plasma arc welding (PAW), laser beam welding (LBW), and electron-beam welding (EBW). However, the equipment cost and the limited flexibility of LBW, EBW and PAW processes restrict their field of application. TIG welding process is most extensively used for the joining of titanium as it produces contamination-free, high-quality welds with good bead appearance. However, the limited penetration capability of TIG process requires groove preparation

and filler wire addition for welding of titanium and other materials more than about 2.5 mm thick. TIG welding over the layer of an activating flux paste to increase the weld penetration was developed by E.O. Paton Electric Welding Institute, Ukraine in the middle of the 1960s, which was later called activated flux TIG (ATIG) welding. Evaporation of the activating flux can provide contraction of the arc column which increases the arc energy density and therefore welding penetration significantly compared to conventional TIG welding [3–5]. ATIG welding has many advantages, viz., (a) welding can be executed using square butt joint geometry and hence no beveling and no filler wire addition, (b) reduced heat input and molten metal volume, (c) reduced residual stress level, and (d) produced distortions free weld joints. Overall, the ATIG process improves the productivity and flexibility, enabling automation of the semi-automatic conventional TIG welding process in which filler metal is added externally.

Active surface tension elements (in general, elements of column VII in the periodic table of elements) reverse the Marangoni convection movements, which are associated with surface tension gradient on the surface of the weld pool. In TIG, Marangoni movements are centrifugal and do not favor the penetration of the weld bead. In ATIG, with active surface tension elements, Marangoni movements become centripetal which enhances the penetration (Fig. 1a). On the other hand, the activating flux may act on the arc physics. The dissociation and ionization of the flux elements may cause arc constriction, which increases arc energy density and therefore welding penetration. It has been found that halides act as surface active elements and they act on the arc physics. Dissociated fluorides have a great affinity with the electrons, which promotes the arc constriction (Fig. 1b) [5, 6].

ATIG fluxes are now available for welding a wide range of materials including carbon steels, low-alloy steels, and stainless steels. However, all the flux formulations are protected by patents. Further, there is a limited study and information available about the ATIG fluxes for welding of Ti and its alloys. The objective of this developmental work is in-house development of activated flux for TIG welding of titanium and qualification of welded joints produced using this flux according to American Society of Mechanical Engineers (ASME) Boiler and Pressure Vessel Code-Section IX requirements and also evaluation of corrosion resistance of this weld joints in boiling nitric acid solution. ASME Section IX covers welding and brazing qualifications.

2 Experimental

2.1 Flux formulation

In the present study, ASTM grade-2 titanium plate of 6 mm in thickness was used to carry out the welding experiments. The chemical composition of the plate is Ti−0.053Fe−0.025O −0.026C−0.006N−0.00002H (weight percent). The titanium base plate used had the following tensile properties: yield strength (0.2 % offset) of 350 MPa, ultimate tensile strength of 402 MPa, and elongation of 41.8 %. To develop the flux formulation, ATIG welding experiments were carried out by autogenous bead-on plate welding. Different metal halide flux powders were chosen to study their influence on arc constriction behavior and on weld penetration. Single and multi-component fluxes were used to optimize the flux formulation. Flux powders ground to very fine powders are mixed with
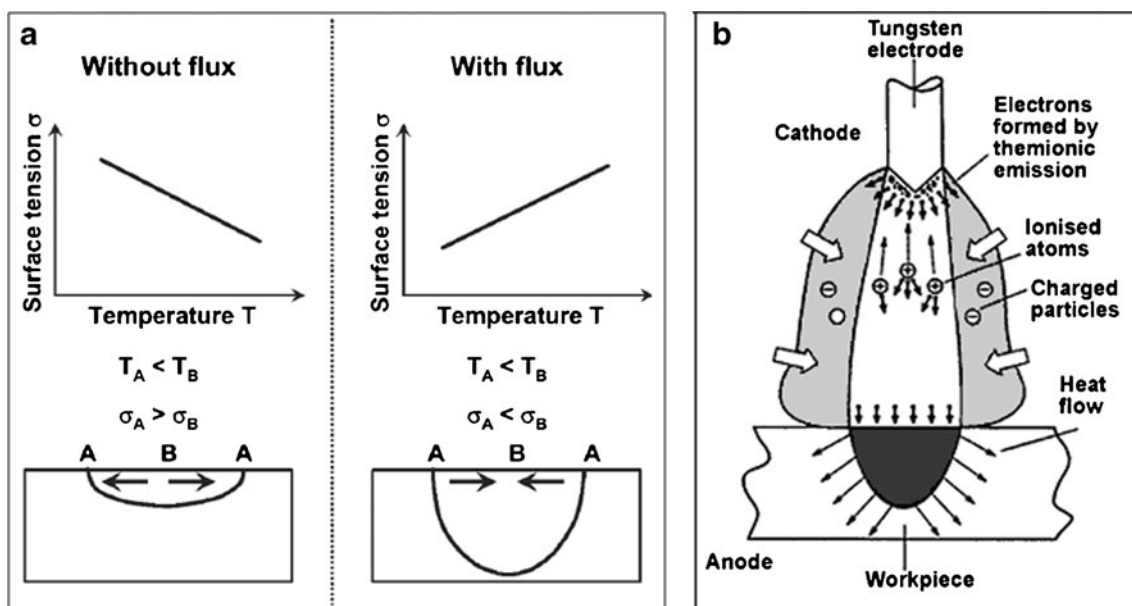

Fig. 1 Mechanism of ATIG welding: **a** Marangoni convection movements and **b** arc constriction

Fig. 2 ATIG welding of titanium in progress

acetone and sodium silicate binder and are applied along the weld line prior to start of welding. Figure 2 shows the ATIG welding experiments in progress using in-house fabricated secondary shielding. The trailing shield protects the weldment from the topside and back purging protects it from the root side. Commercially pure argon was used for the secondary shielding. However, high purity argon and helium was used for primary shielding (torch shielding) which controls the arc characteristic and protects the weld metal and tungsten electrode while welding.

At the beginning, welding experiments were carried out using helium as torch shielding gas. The flux formulation was optimized after doing many trials with different set of flux

powders and metallographic observation of the weld bead profile (bead width and penetration). Welding parameters were optimized to achieve full penetration on a 6-mm-thick titanium plate. Bead on plate welding experiments were carried out for different welding parameters using conventional TIG and ATIG welding process to study the bead profile variation between this two welding processes. To study the effect of argon as shielding gas on the weld bead profile, welding experiments were also carried out with different combination of welding parameters using the developed flux. High-speed camera was used to capture the arc profile in TIG and ATIG welding process.

2.2 Fabrications and testing of ATIG weld joints

Using the developed flux and optimized welding parameters, autogenous ATIG weld joints were fabricated from a 6-mm-thick titanium plate using square-butt joint geometry and helium as shielding gas. Figure 3a, b shows the face side and root side, respectively, of an ATIG weld joint showing consistent weld bead with full penetration on the root side. The joints were qualified by X-ray radiography (Fig. 3c). The strength of the joint was evaluated by tension testing, and ductility of the joint by root bend and face bend test as per ASME Section IX. The corrosion resistance of titanium base material and ATIG weld joint was evaluated in 11.5 M boiling nitric acid solutions. Specimens were prepared metallographically and etched in an aqueous solution containing 10 %

Fig. 3 Autogenous ATIG butt-weld joint: a face side, b root side showing full penetration, and c X-ray radiography image
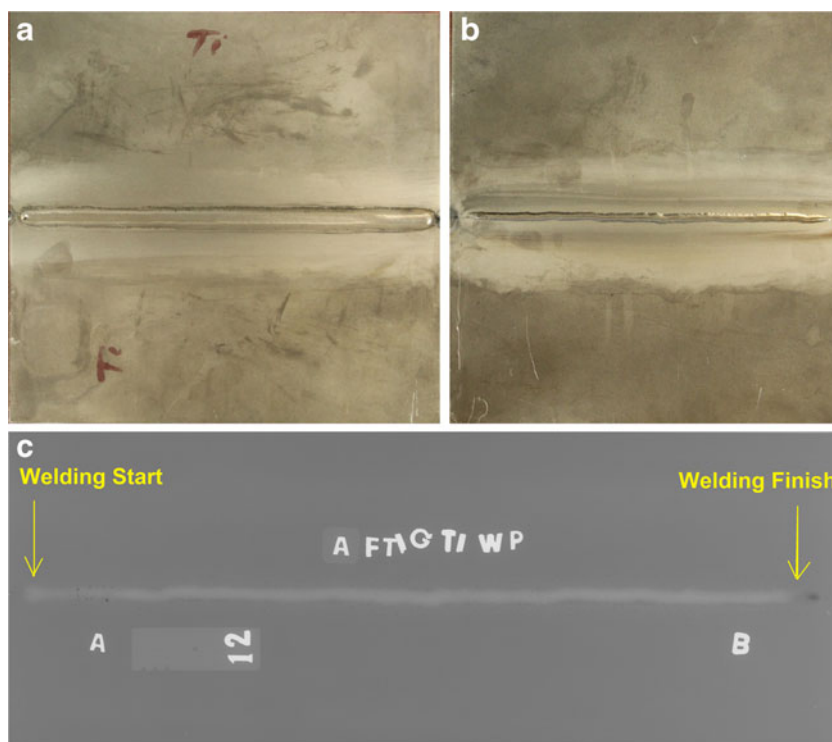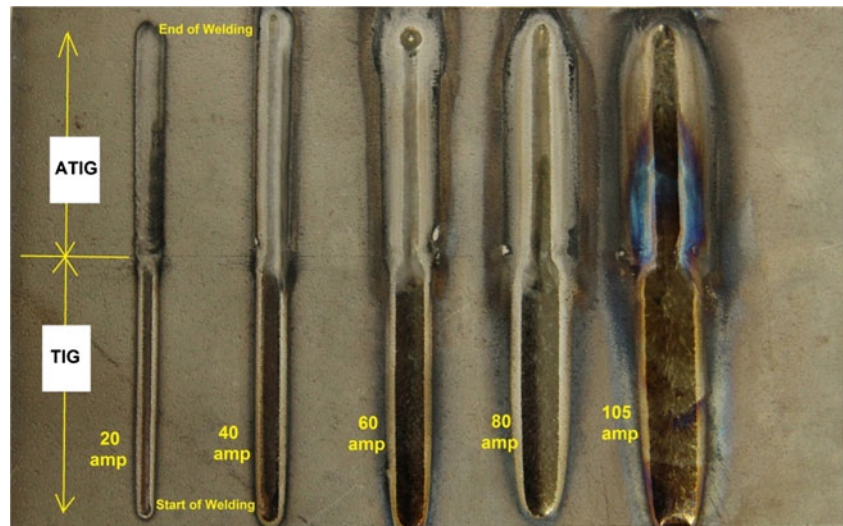
Fig. 4 TIG and ATIG welding of titanium using helium as torch shielding gas using different welding currents

HNO$_3$ and 5 % HF for macro- and microstructure studies. Hardness measurements were carried out across the fusion line at 0.5 mm interval using Vickers Micro-hardness tester with 1 kg load. The microstructure study of the samples was done using light optical microscope.

3 Results and discussion

Figure 4 shows the bead on plate welds of titanium produced by TIG welding and ATIG welding processes using helium as shielding gas. Activated flux was applied on half length of the weld line, and the remaining half length was kept as it is to study the weld profile variation between TIG and ATIG welding process for same welding current. Welding speed of 100 mm/min was maintained constant for all the welding experiment. As shown in Fig. 4, welding started from bare side of the titanium plate and progress towards the flux side without any interruption. It is clear that for the same welding parameter (except for welding current of 20 ampere), there is a substantial reduction in weld bead width in ATIG welding compared to conventional TIG welding which is a clear indication of effectiveness of the used flux which resulted in arc constriction and/or reversal of Marangoni flow in the molten weld pool. For clarity, the magnifying image of Fig. 4 for welding current 80 A is shown in Fig. 5 which clearly shows the change in weld bead profile and bead width reduction while moving from conventional TIG to ATIG welding. However, for welding current of 20 A, there was no melting of the titanium that occurred in ATIG welding in contrast to conventional TIG welding where melting of titanium took place (Fig. 6). In ATIG welding, part of the arc heat is utilized in melting of the flux and the balance heat is used to melt the base material. This shows that the heat generated in 20 A current was fully consumed for melting of the flux, and hence, no melting of the base material took place. The same welding current in conventional TIG welding was able to produce a continuous molten weld pool as the arc heat was directly impinging on the metal surface and used only for the localized heating and melting of the base material. This study shows that ATIG welding process is not effective at very low current level and there is a requirement of minimum threshold heat
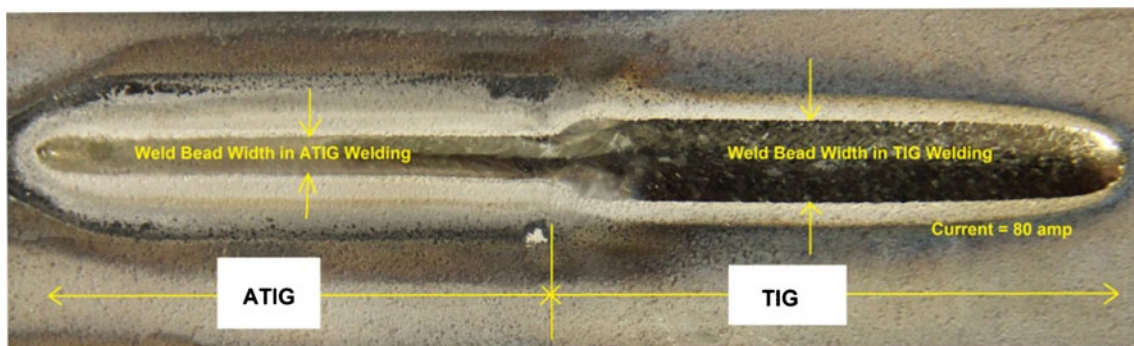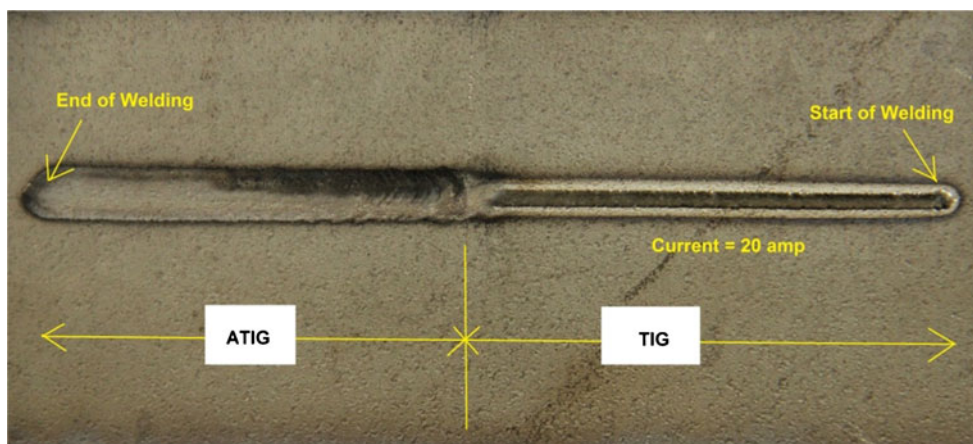

Fig. 5 Magnifying image for welding current of 80 A in Fig. 4

Fig. 6 Magnified image of ATIG weld at 20 A welding current showing no melting of titanium

energy to activate the welding process owing to flux. Table 1 shows the measured weld bead width and penetration in TIG and ATIG bead on plate welds of titanium using helium as a shielding gas. The welding parameters (current=105 A and welding speed=100 mm/min) which produce full penetration weld for a 6-mm-thick plate in ATIG welding process are resulted in only 2.75 mm depth of penetration in the convention TIG welding process. Depth to width ratio of ATIG weld is quite high (1.16) compared to 0.25 of conventional TIG welds. The aforementioned welding parameters were considered as optimized welding parameters for ATIG welding of 6-mm-thick titanium using helium as shielding gas.

Table 2 shows the measured weld bead width and depth of penetration for the different combination of welding parameters with argon as a primary shielding. Figure 7 shows photographs of the weld bead cross section, and the sample identification corresponds to the Table 2. The welding parameters (current=150 A and welding speed=100 mm/min) used for ATIG weld sample E resulted in full penetration weld with

depth of penetration 6.6 mm, while the same welding parameters resulted in only 2.8 mm depth of penetration in the conventional TIG weld sample G. The bead width measured for ATIG welds A to F were in the range of 3.8–5.1 mm compared to about 11 mm for conventional TIG weld. ATIG welding process produces a very narrow weld bead with depth-to-width ratio of around 1.25 compared to 0.25 of conventional TIG welds produced using same welding parameters. As mentioned earlier, when helium is used as a primary shielding, the optimized welding parameters to achieve full penetration on 6-mm-thick titanium are welding current of 105 A and welding speed of 100 mm/min. Thus, use of helium requires lesser welding current (low heat input) compared to argon. This is mainly attributed to the higher ionization potential and thermal conductivity of helium. These properties make helium gas assisted welding arc more powerful and consequently produce deeper penetration with lesser current.

Figure 8 shows the arcs in TIG and ATIG welding processes for the same welding parameter captured using high-speed camera. In TIG welding, the arc is symmetric with circular

Table 1 Variation of weld bead width and penetration for different welding current in TIG and ATIG welding processes using helium as a shielding gas

Welding current (A)	Welding process	Torch shielding	Weld bead width (mm)	Weld penetration (mm)
20	TIG	Helium	2	0.6
	ATIG		No melting	No melting
40	TIG	Helium	4.1	1.35
	ATIG		2.4	2.25
60	TIG	Helium	6.4	1.8
	ATIG		3.5	4
80	TIG	Helium	8.25	2.1
	ATIG		4.2	4.8
105	TIG	Helium	10.82	2.75
	ATIG		5.5	6.4

Table 2 Variation of weld bead width and penetration for different welding current and speed in TIG and ATIG welding process using high purity argon as a shielding gas

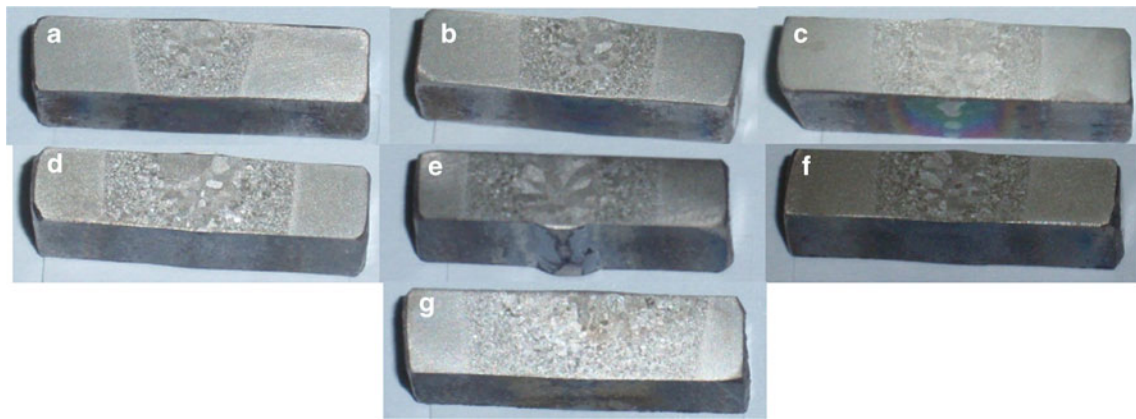| Sample no.	Welding process	Torch shielding	Welding parameters		Weld bead width (mm)	Weld penetration (mm)
			Current (A)	Speed (mm/min)		
A	ATIG	High-purity Argon	105	108	4.1	4
B			120	108	4.1	5.5
C			130	100	4.75	5.7
D			140	100	5	5.8
E			150	100	5.1	6.6
F			110	75	3.8	5.6
G	TIG		150	100	11	2.8

Fig. 7 Macrograph of the weld beads with different welding parameters. Samples *A–F* are ATIG welds, while sample *G* is normal TIG weld

curvature at the bottom (Fig. 8a). While in ATIG welding, the arc is asymmetric and flat at the contact point with the plate surface (Fig. 8b). In ATIG welding, the arc is constricted on the leading side (front) compared to diffusible arc (arc spread) on the trailing side (back). As welding progress, the flux is melted and vaporized by the arc heat on the leading side and there will be no flux on the trailing side of the arc. Therefore, there was no sign of arc constriction on the trailing side and the arc is diffusible similar to conventional TIG welding. The arc constriction on the leading side and overall arc size reduction in ATIG compared to TIG is a proof of mechanism of arc constriction by the used flux which increases the arc energy density and therefore welding penetration.

Figure 9 shows formation of coarse and mostly columnar prior β grains (bcc structure) while weld solidification in TIG as well as ATIG welding process. The weld metal structure (Fig. 9a, b) was taken in the as-welded condition without polishing and without etching as the structure was already thermally etched. The weld metal microstructure shows presence of acicular α (HCP structure) formed by nucleation and growth along several sets of planes within each prior β grain and its basket-weave appearance is characteristic of Widmanstatten structure (Fig. 9d). Figure 10 shows the microstructure of titanium base

metal and heat affected zone of ATIG weld joint. The base metal shows fine equiaxed α grains (HCP structure), while the heat affected zone shows coarse equiaxed prior β grains and the grain size increases towards the fusion line. Also, the heat affected zone shows the presence of acicular α formed by nucleation and growth along several sets of planes within each prior β grain similar to weld metal structure.

Figure 11 shows the hardness profile across the fusion line. There is no noticeable variation in hardness among base metal, heat-affected zone, and weld metal which indicates that the weld was not contaminated by components of flux or atmospheric gases which could result significant increased in hardness of the weld metal leading to embrittlement.

Table 3 shows the transverse tension test results of ATIG weld joints. The average ultimate tensile strength and elongation of two tests is around 398 MPa and 21.5 %, respectively, and both the samples fractured in weld metal (Fig. 12). However, the weld metal shows ductile mode of fracture and the tensile strength of the weld joint is close to the base material tensile strength of 402 MPa. Also, the tensile strength of the weld joint is well above the minimum specified tensile strength of 345 MPa for ASTM grade-2 titanium base material, and hence, the tensile properties of the ATIG weld joints

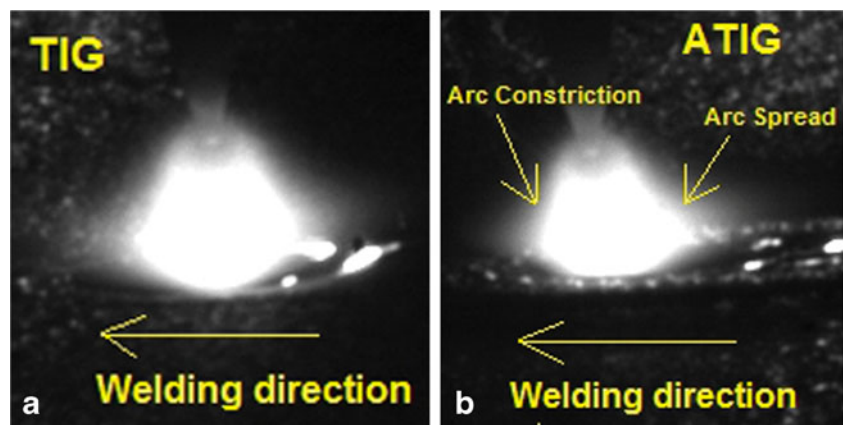**Fig. 8** **a** TIG and **b** ATIG welding arcs captured using high-speed camera

Fig. 9 Weld metal microstructure of titanium produced by TIG (**a**, **c**) and ATIG (**b**, **d**) welding process. Microstructures (**a** and **b**) are without polishing and without etching, and (**c** and **d**) are with polishing and etching
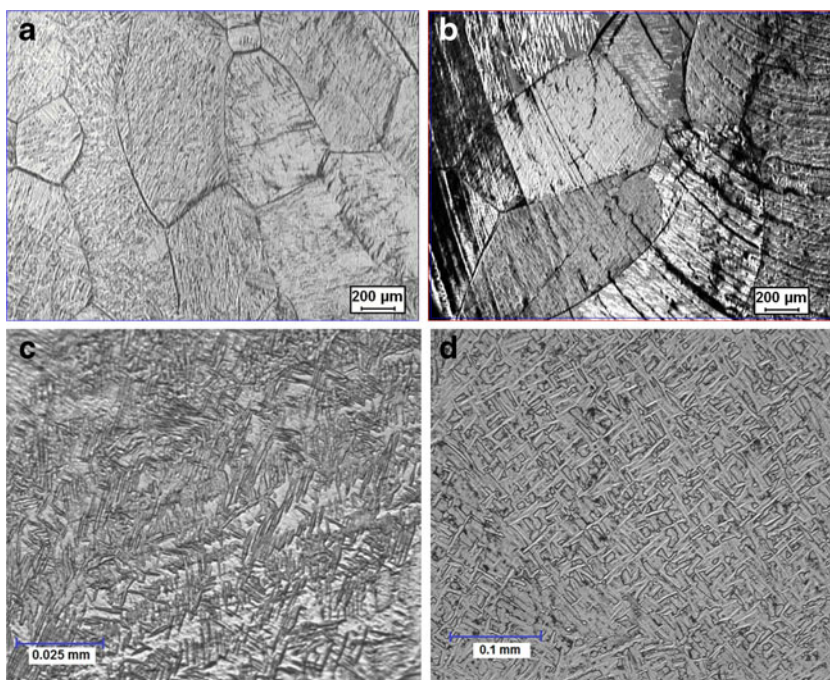
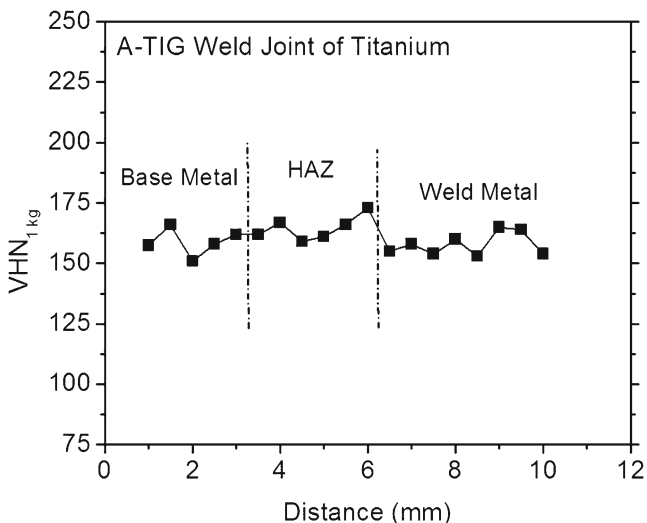**Fig. 10** Optical micrographs of titanium: **a** base metal and **b** and heat affected zone of ATIG weld joint
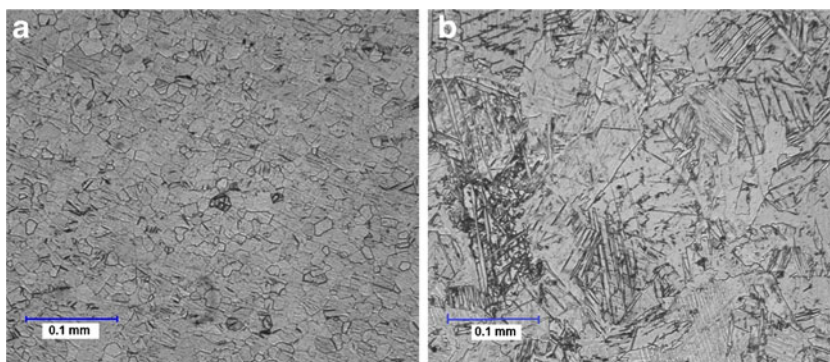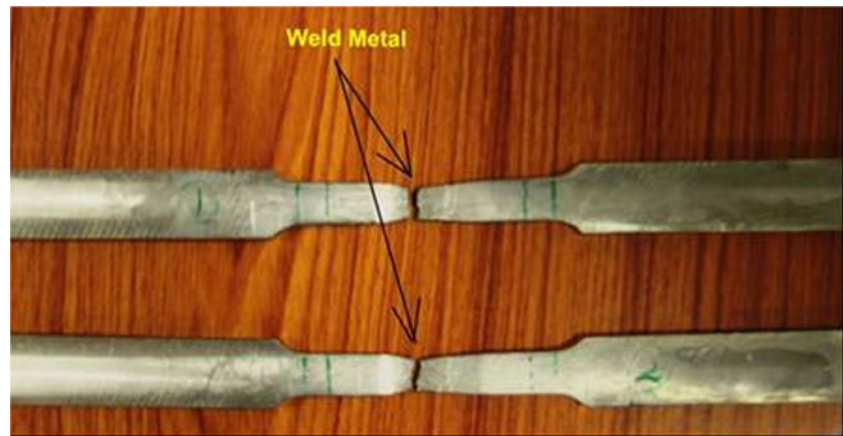
Fig. 11 Hardness profile across the fusion line of ATIG weld joint

Table 3 Tension test results of ATIG weld joints

Properties	Tensile strength (MPa)	% of elongation (gage length=50 mm)	Failure location
Test 1	398.2	21.3	Weld
Test 2	397.6	21.8	Weld

are acceptable as per ASME Section IX. The failure in the weld metal could be due to the presence of coarse primary β grains in the weld metal. The root bend and face bend tests passed 4T bend radius as per ASME Section IX requirements with bend angle of 180° which show joints are ductile (Fig. 13).

As mentioned earlier, titanium is a candidate material in nuclear industries for the reprocessing of spent fuel where nitric acid in boiling condition is used for the dissolution of the spent fuel. Therefore, the corrosion resistance of titanium and its weld joints in boiling nitric acid are important which governs the service life and safe operation of the equipments. Titanium base materials and its ATIG weld joints were subjected to three phase corrosion tests (liquid, vapor, and condensate phase) in nitric acid bath of 11.5 M concentration [7]. The concentration of the acid was selected as 11.5 M to simulate the acid concentration used in the fuel reprocessing plant. The three-phase corrosion testing was carried out using the apparatus as shown in Fig. 14. The apparatus was so designed that when 11.5 M nitric acid was used in the liquid phase, the equilibrium concentration in the condensate phase was 6.0 M.

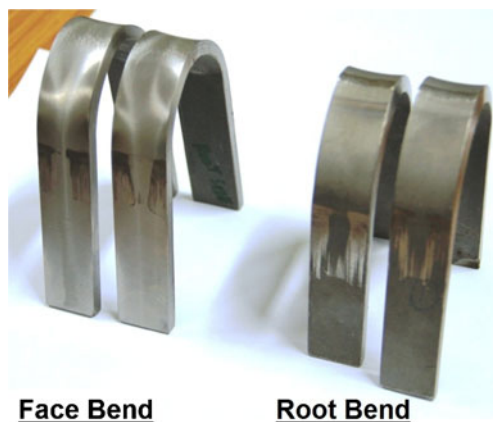Samples for corrosion study were machined out from titanium base material and ATIG weld joints and were polished up to 600 grit emery papers. The rinsed and dried samples were weighed and the initial dimensions recorded for exposed surface area determination. The samples were suspended in the liquid, vapor, and condensate phase using Teflon (PTFE) thread as shown in the Fig. 14 and exposed for a total period of 240 h. After every 48-h period, the samples were removed and the changes in the weights recorded, and fresh test solution was used for each period. After completion of the test, the average corrosion rate for five individual periods was calculated. Table 4 shows the average corrosion rates for 240 h for the Ti base material in liquid, vapor, and condensate phases of
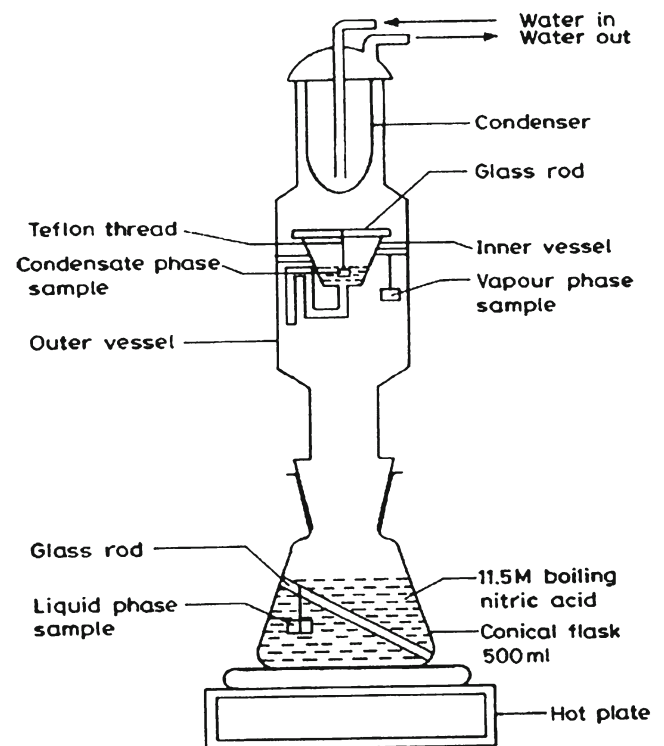

Fig. 13 Bend test samples of ATIG weld joint

Fig. 14 Schematic of experimental setup for three-phase corrosion testing

Table 4 Corrosion rate of titanium and its weld joints in 11.5 M boiling nitric acid

Material condition	Corrosion rate (mpy)		
	Liquid	Vapor	Condensate
Titanium base material	15.17	0.366	0.3
ATIG weld titanium	11.90	0.62	0.76

boiling 11.5 M nitric acid. The corrosion rate of base material and weld joint is more in liquid phase due to high concentration of nitric acid in the liquid bath compared to the vapor and condensate phases. Therefore, the corrosion rate of titanium base material and weld joint in liquid phase governs the thickness of the vessel to be used for a designed service period. The corrosion resistance of the weld joint is superior to base material in liquid phase. Based on this corrosion study, it is confirmed that the weld joints produced using the developed flux is having no adverse affect on the corrosion resistance of the weld joint and hence can be used for application where the weld joints will be exposed to nitric acid solution.

Figures 15 and 16 show corrosion tested samples of titanium base material and weld joint, respectively. In ATIG welding, the weld metal is the portion of the base materials on either side of the joint line which was melted by the TIG arc and subsequently solidifies and there is no use of external filler wire. So, there is no chemistry difference between weld metal and base material. The main difference between weld metal and base material is their microstructure which has been shown explained earlier (Figs. 9 and 10). The liquid phase corrosion of titanium base material is almost uniform throughout the specimen surface (Fig. 15). While in case of weld joint, there is some noticeable difference in corrosion attack between weld metal and base material regions of the specimen in liquid phase and base metal region is more attacked compared to weld metal (Fig. 16). As there is no chemistry difference between weld metal and base material, the microstructure difference could be the possible reason for differential corrosion attack between weld metal and base material regions. The microstructure difference between

weld metal and base material might have created a galvanic cell and hence lead to differential corrosion attack. However, overall corrosion loss of weld joint is less compared to titanium base material in liquid phase which is clearly revealed in their photographs (Figs. 15 and 16). In reverse, the corrosion rate of titanium base material is less compared to weld joint in vapor and condensate phases. The concentration of nitric acid in the vapor and condensate phases are less compared to liquid phase and the corrosion attack may vary/alter for a particular microstructure with change in concentration of nitric acid and hence lead to difference in corrosion loss.

The photographs of base material and weld joint specimens tested in vapour and condensate phases (Figs. 15 and 16) clearly revealed that there is no noticeable corrosion attack and the specimens looked like parent material prior to testing. The corrosion loss in the range of 0.3–0.76 mpy found for base material and weld joints in vapor and condensate phases are very less and negligible with respect to liquid phase corrosion rate of 11.9–15.17 mpy for the nitric acid application.

4 Conclusion

The activated flux for TIG welding of titanium was successfully developed, and the developed flux is capable of producing full penetration weld on 6-mm-thick titanium in a single pass. The ATIG welding process produces a very narrow weld bead with depth-to-width ratio of around 1.25 compared to 0.25 of conventional TIG welds produced using same welding parameters.

1. ATIG welding was successfully demonstrated in joining of 6-mm-thick titanium plates using square-butt joint geometry in a single pass and the weld joints passed X-ray radiography.
2. The root bend and face bend tests passed 4T bend radius as per ASME Section IX requirements with bend angle of 180° which indicate that the joints are ductile. The transverse tensile testing of the weld joints fractured in the weld metal with tensile strength of 398 MPa with

Fig. 15 Corrosion tested specimens of titanium base material in three different phases
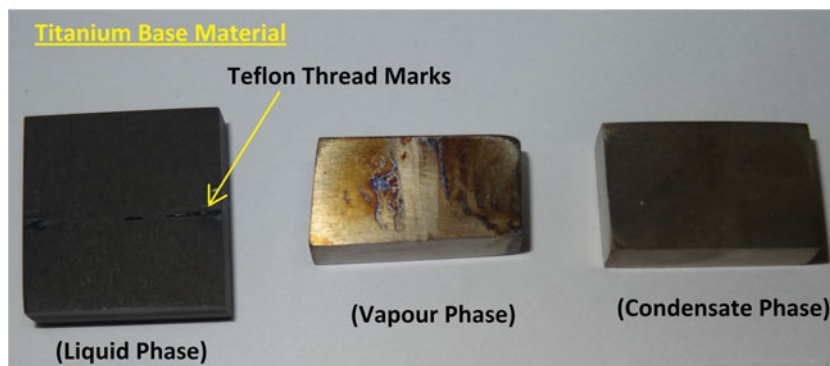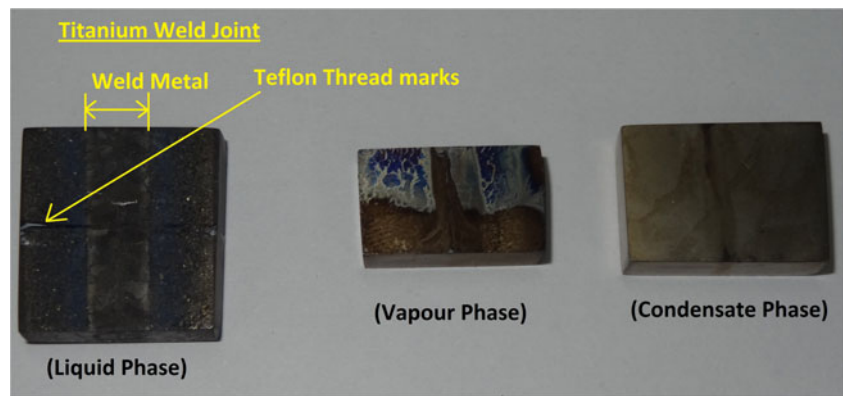
Fig. 16 Corrosion tested
specimens of titanium weld joints
in three different phases

sufficient ductility. The failure in the weld metal could be due to the presence of coarse and columnar primary β grains in the weld metal. However, the tensile strength of the weld joint is closer to the base material tensile strength of 402 MPa and met the ASME Section IX requirements.

3. The corrosion rate of base material and weld joint is more in liquid phase due to high concentration of nitric acid in the liquid bath compared to the vapor and condensate phases. Therefore, the corrosion rate of titanium base material and weld joint in liquid phase governs the thickness of the vessel to be used for a designed service period. The corrosion resistance of the weld joint is superior to base material in liquid phase. Based on this corrosion study, it is confirmed that the weld joints produced using the developed flux is having no adverse affect on the corrosion resistance of the weld joint and hence can be used for application where the weld joints will be exposed to nitric acid solution.

References

1. Baeslack WA, Davis JR, Cross CE (1993) Selection and weldability of conventional titanium alloys', 10th ed. ASM Handbook 6:507–523
2. Terrance, R Welding of titanium alloys: ASM Handbook, 10th ed., Vol. 6, pp.783–786
3. Tanaka M, Shimizu T, Terasaki H, Ushio M, Koshi-ishi F, and Yang CL (1993) Effects of activating flux on arc phenomena in gas tungsten arc welding, Science and Technology of Welding and Joining 2000, Vol.5, No.6, PP. 397–402
4. Shamping LU, Hidetoshi Fujii, Hiroyuki Sugiyama, Manabu Tanaka and Kiyoshi Nogi (2003) Marangoni Convection and Welding Penetration in A-TIG Welding, Trans. JWRI, Vol.32, No.1
5. Lowke JJ, Tanaka M, Ushio M (2005) Mechanisms giving increased weld depth due to a flux. J Phys D: Appl Phys 38:3438–3445
6. Leconte S, Paillard P, Chapelle P, Henrion G, Saindrenan J (2007) Effects of flux containing fluorides on TIG welding process. Sci Technol Weld Join 12(2):120–126
7. Furuya T, Kawafuku J, Satoh H, Shimogori K, Aoshima A, Takeda S (1991) A corrosion testing method for titanium in nitric acid environments. ISIJ Int 31(2):189–193